Published in final edited form as:
Neuroimage. 2011 March 15; 55(2): 468–478. doi:10.1016/j.neuroimage.2010.12.032.

Age-Associated Reductions in Cerebral Blood Flow Are Independent from Regional Atrophy

J. Jean Chen[1,2], **H. Diana Rosas**[1,3], and **David H. Salat**[1,2,4]

[1]MGH/MIT/HMS Athinoula A. Martinos Center for Biomedical Imaging, Massachusetts General Hospital, Harvard Medical School

[2]Department of Radiology, Massachusetts General Hospital, Harvard Medical School

[3]Department of Neurology, Massachusetts General Hospital, Harvard Medical School

[4]Neuroimaging Research for Veterans Center, VA Boston Healthcare System

Abstract

Prior studies have demonstrated decreasing cerebral blood flow (CBF) in normal aging, but the full spatial pattern and potential mechanism of changes in CBF remain to be elucidated. Specifically, existing data have not been entirely consistent regarding the spatial distribution of such changes, potentially a result of neglecting the effect of age-related tissue atrophy in CBF measurements. In this work, we use pulsed arterial-spin labelling to quantify regional CBF in 86 cognitively and physically healthy adults, aged 23 to 88 years. Surface-based analyses were utilized to map regional decline in CBF and cortical thickness with advancing age, and to examine the spatial associations and dissociations between these metrics. Our results demonstrate regionally selective age-related reductions in cortical perfusion, involving the superior-frontal, orbito-frontal, superior-parietal, middle-inferior temporal, insular, precuneus, supramarginal, lateral-occipital and cingulate regions, while subcortical CBF was relatively preserved in aging. Regional effects of age on CBF differed from that of grey-matter atrophy. In addition, the pattern of CBF associations with age displays an interesting similarity with the default-mode network. These findings demonstrate the dissociation between regional CBF and structural alterations specific to normal aging, and augment our understanding of mechanisms of pathology in older adults.

Keywords

Cerebral blood flow (CBF); aging; arterial-spin labelling (ASL); magnetic resonance imaging (MRI); quantitative perfusion; Alzheimer's disease; dementia; cortical thickness; cerebral cortex

INTRODUCTION

Continuous and sufficient cerebral blood flow (CBF) is vital to neural function; thus, cerebral perfusion, typically quantified by measuring the volume of blood passing through

Corresponding Author: J. Jean Chen, A. A. Martinos Center for Biomedical Imaging, 149 13th Street Room 2241, Massachusetts General Hospital, Harvard Medical School, Charlestown, MA, U. S. A. 02129, jjchen@nmr.mgh.harvard.edu.

the microvascular network in a given volume of tissue over a certain duration, is a key indicator of cerebral health. It has long been established that CBF is normally coupled to cerebral oxygen ($CMRO_2$) and glucose consumption in steady state (Hoge et al., 1999; Sokoloff et al., 1977). Disruption of this system may suggest compromised vascular function and/or abnormal metabolism. It is therefore not surprising that reduced CBF and disrupted neurovascular coupling are associated with numerous pathological conditions, such as hypertension, ischemic stroke, and Alzheimer's disease (Girouard and Iadecola, 2006; Gsell et al., 2000). However, it is not fully understood if changes in CBF arise in normal aging, and whether such changes are associated with the well described tissue atrophy in older adults.

The brain undergoes a wide array of anatomical and functional changes in normal aging (Morrison and Hof, 1997), associated with an increasing risk of age-related neurovascular diseases that compromise the functional integrity of the neurological system. A number of epidemiological (Aguero-Torres et al., 2006; Breteler, 2000; Ruitenberg et al., 2005), pharmacotherapeutic (Duron and Hanon, 2010; Forette et al., 2002; Tzourio et al., 2003), and neuroimaging studies (Alsop et al., 2008; Dai et al., 2008c, 2009; Uh et al., 2009) suggest vascular contributions to Alzheimer's disease (AD) and other dementia (Bell and Zlokovic, 2009; Caroli et al., 2007; de la Torre, 2005; Dickstein et al., 2010; Helzner et al., 2009; Ruitenberg et al., 2005; Sachdev et al., 1999; Zlokovic, 2005). Thus, understanding changes in blood flow in cognitively healthy older adults may be an important step towards differentiating normal from abnormal alterations in physiology (Elias et al., 1995; Farmer et al., 1990; Nagata et al., 2000; Skoog et al., 1996). Regional hypoperfusion has been found to be associated with amyloid accumulation (Driscoll et al., 2010; Sojkova et al., 2008) as well as cognitive deficits (Alves and Busatto, 2006). The reported links between perfusion reduction, neuronal damage and structural deterioration (Fierstra et al., 2010; Tohgi et al., 1998) beg the question of how aging-associated CBF reductions relate to the wide-spread cerebral atrophy (Akiyama et al., 1997; Buckner et al., 2004; Raz et al., 1997; Salat et al., 2004), and more critically, which changes are not secondary to normal aging but may instead indicate impending pathology. Invaluable clues can be gleaned by integrating quantitative perfusion and anatomical imaging,

Perfusion imaging has conventionally been performed using positron-emission tomography (PET) (Beason-Held et al., 2009; Meltzer et al., 2000; Pantano et al., 1984), single-photon emission computed tomography (SPECT) (Alves and Busatto, 2006; Inoue et al., 2005; Yang et al., 2002), X-ray computed tomography (CT) (Akiyama et al., 1997; Meyer et al., 1994) and contrast-enhanced MRI (Helenius et al., 2003). Arterial-spin labelling (ASL) (Detre et al., 1998; Oguz et al., 2003; Parkes et al., 2004; Williams et al., 1992; Wong et al., 1997) is a relatively novel and minimally invasive perfusion methodology requiring no exogenous tracers, and continuous ASL (CASL) (Detre et al., 1998; Detre et al., 1992; Detre et al., 1994) as well as the more novel pseudo-continuous ASL (Dai et al., 2008b; Silva and Kim, 1999) have recently found application in clinical populations (Alsop et al., 2008; Alsop et al., 2010; Detre et al., 1998; Xu et al., 2010). However, regional CBF changes in cognitively healthy adults specific to the full adult life-span remains to be clarified. In this work, we examine the effects of normal adult aging on CBF using advanced anatomical models and morphological procedures which permitted the assessment of regional alterations in cortical and subcortical tissue. We used pulsed ASL in conjunction with high-resolution structural MRI to evaluate regional cortical and subcortical resting CBF measures in cognitively healthy older adults. Unique to this study is the mapping of MRI measurements of age-associations in CBF in relation to regional brain atrophy in a cortical surface-oriented manner. This procedure permitted detailed examination of the association between age-related changes in CBF and tissue volume, as well as the reduction of the potential influence of partial volume contamination on the CBF values. We found that

reductions in CBF were independent of concurrent age-related tissue volume reduction, as perfusion can remain unaltered in regions of significant tissue atrophy. This apparent "dissociation" suggests that tissue shrinkage and hypoperfusion may not take place concurrently. Our findings underscore the importance of perfusion and structural measures as individually unique metrics of neurological changes in aging.

MATERIALS AND METHODS

Participants

This study involved 86 cognitively healthy participants, (38 men/48 women), aged from 22.9 to 88.2 years. These were subdivided into young (YA, age < 40), middle-aged (MA, 40 ≤ age < 60) and older (OA, age ≥ 60) adult groups. Younger adults were recruited through the MGH and local community, and older adults were recruited through the Harvard Cooperative Program on Aging (http://www.hebrewrehab.org/home_institute.cfm?id=90) and the Nurses' Health Study (http://www.channing.harvard.edu/nhs/) at Harvard Medical School and Brigham and Women's Hospital as well as the local community. Older adults were screened for dementia using the Mini Mental Status Exam (MMSE) (Folstein et al., 1975), with a minimum MMSE requirement of 24. We also included scores from the National Adult Reading Test (ANART) (Grober and Silwinski, 1991) and the Hopkins Verbal Learning Test (HVLT) (Vanderploeg et al., 2000) as indicators of cognitive health, as well as the Geriatric Depression Scale (GDS) for psychiatric health (Yesavage et al., 1982). Demographic information is provided in Table 1. Education levels were matched in all age groups. We excluded individuals with signs of major neurologic or psychiatric illnesses outside the range of vascular conditions in our inclusion criteria (mild forms of hypertension, hyperlipidemia, and diabetes). History of diabetes or high blood pressure was noted. Conditions for exclusion included dementia, high cerebrovascular disease risk, cancer of the central nervous system, major head trauma, overt cerebrovascular disease (including stroke and hemorrhage), and other neurological or psychiatric conditions that would be expected to influence cognition or imaging measures including human immunodeficiency infection (HIV), hydrocephalus, brain tumors, sarcoidosis, and multiple sclerosis. We also excluded individuals taking medications that would be expected to have a substantial effect on cognitive abilities. Experiments were performed with the understanding and written consent of each participant, according to the Institutional Review Board guidelines.

MRI Acquisition

All images were acquired using a Siemens Trio 3 Tesla system. The scans employed 12-channel phased-array head coil reception and body-coil transmission. A 3D anatomical was acquired using multi-echo MPRAGE (van der Kouwe et al., 2008), with resolution 1 × 1 × 1 mm, TR = 2530 ms, TI = 1000 ms, TE = 1.64, 3.50; 5.36 and 7.22 ms, field of view = 256×256 mm (sagittal), matrix size = 256×256×176, bandwidth = 651 Hz/pixel, and GRAPPA factor = 2.

Two PASL datasets were obtained sequentially for each subject using the FAIR QUIPSS II PASL technique (Wang et al., 2002). A slice-selective frequency-offset corrected inversion (FOCI) pulse was applied during tag and control, the latter scan acquired in the absence of slab-selective gradients. The tag and control labelling thicknesses were 140 mm and 340 mm, respectively, leaving 100 mm margins at either end of the imaging slab to ensure optimal inversion profile. The QUIPSS II saturation pulse was applied to a 100 mm slab inferior to the imaging region with a 10 mm gap between the adjacent edges of the saturation and imaging slabs. Flow crusher gradients were applied with a threshold of 100 cm/s. Other imaging parameters were: 64 × 64 matrix, 24 slices (ascending interleaved acquisition), with a voxel size = 3.4 × 3.4 × 5 mm^3. The slice positioning and sample FAIR

images area shown in Figure 1. The PASL acquisitions each consisted of 104 frames (52 tag and 52 control), with TI1 = 600 ms and TI2 = 1600 ms, chosen to accommodate a wide range of flow rates. The scans used a repetition time (TR) of 4 s, and an echo-time (TE) of 12 ms, made possible by the current implementation of ¾ partial Fourier echo-planar imaging (EPI) readout, which enabled the minimization of BOLD effects and the reduction of susceptibility-related geometric distortions. The acquisition time per slice was 42 ms. A 2D gradient-echo EPI (echo-planar imaging) sequence was used in a calibration scan (with TR set to 10 s) to estimate the equilibrium magnetization of arterial blood. Sample images from the ASL acquisition is presented in Figure 1.

Data Processing

Structural Assessments—All structural assessments were performed on the multi-echo MPRAGE images using the FreeSurfer image processing and analysis package (publically available at http://surfer.nmr.mgh.harvard.edu). The procedure includes removal of non-brain tissue using a hybrid watershed/surface deformation procedure (Segonne et al., 2004), automated transformation into the MNI152 standard space, intensity normalization (Sled et al., 1998), tessellation of the grey matter white matter boundary, automated topology correction (Segonne et al., 2007), and surface deformation following intensity gradients to optimally place the grey/white and grey/CSF borders at the location where the greatest shift in intensity defines the transition to the other tissue class (Fischl and Dale, 2000). The subsequent segmentation of the cortex and subcortical grey matter volumetric structures were performed for each subject based on probabilistic models of tissue magnetic resonance parameters and of anatomical locations (Fischl et al., 2004a; Fischl et al., 2004b). The resultant cortical models permitted surface inflation (Fischl et al., 1999a) and registration to a spherical atlas, whereby individual cortical folding patterns were used to match cortical geometry across subjects (Fischl et al., 1999b). Spherical registration has demonstrated superior accuracy than volume-based registration in aligning histological properties (Fischl et al., 2008).

Representations of cortical thickness, calculated as the closest distance from the grey/white boundary to the grey/CSF (cerebrospinal fluid) boundary at each vertex on the tessellated surface (Fischl and Dale, 2000), were produced using segmentation and deformation procedures based on both intensity and continuity information from the entire three dimensional MR volume. The resultant maps are sensitive to sub-millimeter differences in thickness between groups, and have been validated against histological analysis (Rosas et al., 2002) and manual measurements (Salat et al., 2004).

Quantitative CBF Computation—The raw PASL time-series were motion- and drift-corrected using FLIRT (publically available at http://fsl.fmrib.ox.ac.uk/fsl/flirt), and subsequently divided into 52 tag-control pairs per acquisition. To minimize BOLD-contamination, the tag-control difference images were calculated using surround subtraction (Lu et al., 2006). Longitudinal (T_1) relaxation during the slice-dependent transit delays was compensated based on the per-slice acquisition time. The PASL volumes were then averaged across time and across the two datasets to maximize signal-to-noise, following which quantitative CBF maps were obtained according to the single-compartment Standard Kinetic Model (Buxton et al., 1998). The equilibrium arterial-blood magnetization was computed as the intensity in the calibration scan adjusted for longitudinal (T_1) and transverse relaxation (T_2^*) differences as well as blood-tissue water partition coefficient (λ). Typical values for proton density, λ, T_1 and T_2* were assumed for all grey matter based on prior literature, as described in (Čavuşoğlu et al., 2009). The labeling efficiency was assumed to be 98% (Wong et al., 1998).

Group Analysis—To enable surface and ROI-based analyses, the PASL data were upsampled to 1 mm^3 spatial resolution and registered to the native-space anatomical images using boundary-based registration (Greve and Fischl, 2009). Specifically, the mid-frame of the motion- and drift-corrected PASL time-series was chosen as the template image, and cross-modality registration was achieved by minimizing the misalignment between the cortical grey-white boundaries in the anatomical and PASL template images through 12 degree affine transforms. This method is minimally sensitive to differences in contrast and intensity non-uniformity in the two datasets, and the procedure benefited from the reduced geometric distortions in the PASL images through the short-TE partial-Fourier acquisition.

All segmentation-based volume ROIs were eroded by 1 mm around the perimeter to further reduce partial-volume contamination. Mean CBF values across volume ROIs were computed in native space, and regressed against age, both with and without using structural volume as a covariate. Cortical CBF reductions with age were assessed across the cortex and separately in the hippocampus. In addition, resting CBF in all cortical parcellations (Fischl et al., 2004b) was compared across hemispheres, genders and age-groups using multi-variate ANOVA.

To facilitate group-analysis, the anatomical-registered PASL data were sampled onto a surface atlas using spherical registration. The surface-sampling of the upsampled CBF maps was performed at a depth of 50% into the cortical ribbon. This approach was favoured over the inclusion of the entire cortex, despite the large voxel size in the source CBF images, as it was found to reduce the inclusion of voxels contaminated with white-matter or CSF. It was further cross-validated using the ROI-based approach described below. Group-mean CBF maps were generated using non-rigid high-dimensional spherical averaging (Fischl et al., 1999a). The interaction between cortical CBF and age was assessed by regressing out concurrent variations in cortical thickness, out of consideration for atrophy-related partial-volume contamination of CBF measures. Outliers were removed based on the standardized residuals (exclusion criterion = 2 standard deviations) prior to the regression analyses. General linear model-based statistical tests were performed with smoothing along the cortical surface using a circularly symmetric Gaussian kernel with a full-width at half-maximum (FWHM) of 10 mm, and the results were corrected for multiple comparisons using the false-discovery rate method (Genovese et al., 2002).

To visualize the interplay between resting CBF and thickness in aging-related changes, spatial overlaps were generated from regions showing higher-than-average cortical CBF and/or thickness, and from those showing significant CBF reduction and/or cortical thinning. In addition, regions exhibiting the most significant age-associated CBF reduction were demarcated and analyzed individually, after regressing out variations in cortical thickness. To assess laterality effects (see Supplementary Materials), these regions were labelled ipsilaterally and matched to regions on the contralateral side. For this purpose, the surface labels were converted back into volume space through an extension into the cortical ribbon a depth of 10% to 90%. Furthermore, the thalamus, amygdala and accumbens, as well as substructures of the basal ganglia, were individually segmented, and their respective mean CBF values extracted for both hemispheres. Inter-hemispheric comparisons of CBF and grey-matter volume were also performed for all cortical and subcortical structures. All structural volume measures were corrected for estimated total intracranial volume (eTIV) using the atlas-scaling and covariance approach (Buckner et al., 2004). The significance of the regressions was computed using *t*-tests, and that of the inter-group comparisons were all performed using multi-factorial analysis of variance (ANOVA), with gender and/or age being the potential covariates.

Reproducibility Analysis—Within-session cross-run reproducibility of the quantitative CBF measurements was assessed using the two PASL acquisitions acquired per subject, and quantified through the percent difference, that is, the absolute difference between the CBF values obtained from the two runs normalized by the cross-run CBF mean. In addition, to assess the reliability of the spatial localization of the cortical-thickness and CBF variations with age, we separated the full dataset (from all subjects) into two independent subsets of matched mean ages and sex ratios. One of these was used for the statistical analysis, based on the results of which regions of interest (ROIs) were delineated, and then mapped to the second subset. This methodology permitted us to assess and minimize cohort-specific effects in the observed CBF-age relationship.

RESULTS

Effect of Age on Global CBF

The mean CBF value across the entire cortical grey matter volume was 52.6 ± 9.3, 52.0 ± 10.7, and 42.7 ± 8.8 ml/100 g/min in the young (YA), middle-aged (MA) and older (OA) adult groups, respectively. No significant difference was found between the YA and MA, but these latter were both found to differ from the OA group. The mean subcortical CBF, taken across the amygdala, accumbens, caudate, globus pallidus, putamen and thalamus, was 40.5 ± 7.6, 41.7 ± 7.1, and 39.5 ± 6.2 ml/100 g/min, respectively. One-tailed *t*-test revealed cortical CBF to exceed subcortical CBF in the YA ($p < 0.001$), MA ($p < 0.01$) but not the OA ($p = 0.15$). Also, while there were no differences in mean CBF across hemispheres cortically ($p = 0.90$) and subcortically ($p = 0.91$), laterality effects were observed when examining selected cortical regions (Table 2).

Spatial heterogeneities in CBF were also present, as seen in Figure 2. The mean quantitative CBF values were mapped onto semi-inflated lateral (top) and medial (bottom) surface models in the YA, MA, and OA groups, as shown in Figure 2(a-c). The spatial variation in CBF was similar across age-groups, with OA exhibiting visibly reduced mean CBF compared both YA and MA, and the latter two showing a less remarkable mutual difference. There was also a spatially distinct pattern of variance in the CBF measurements (Figure 2e). Lastly, we also illustrate the relationship between regional cortical thickness and colocalized CBF across individuals (Figure 2f).

We evaluated the association between global CBF, tissue volume and age. Averaging across the entire cortex (encompassing both regions affected and unaffected by age), CBF was found to decrease at 0.38% per year ($p = 0.014$) (Figure 3a), amounting up to 27% over a 70-year period of adult life. In contrast, the slope for cortical volume vs. age (Figure 3b) was 0.85% per year ($p = 5.5\times10^{-8}$). Regression across all subcortical grey-matter structures as a whole revealed minimal decrease with age (Figure 3c), although extensive negative correlations between tissue volume and age were observed across all subcortical structures studied (Figure 3d). No significant pair-wise differences in global mean CBF were found among the age-groups, as shown by the group-average plots in Figure 4. Cortical CBF was higher in women in the OA group ($p < 0.05$) but not in the YA or MA groups. Although no statistically significant gender-disparity was found when all ages were pooled, subsequent statistical analyses examined effects controlled for sex.

Finally, lateralization and sex differences in CBF are presented in Table 2. In general, resting CBF was higher in the right hemisphere and in women (see Supplementary Materials).

Regional Effects of Age on CBF

Regional CBF values averaged across distinct cortical parcellations for the three age groups are shown in Table 2. The caudal middle-frontal, isthmus/posterior cingulate and pericalcarine regions were associated with higher CBF than the cortical average in all groups, although the differences were not statistically significant. ANOVA indicated a myriad of cortical parcellations displaying reductions in CBF in the OA as compared to the MA. In contrast, fewer regions exhibited such effects in the MA compared to the YA. Similar group trends pertain to the subcortical structures (Table 2), with Figure 5 showing gender-dependence in individual parcellations. In the regression against age (Table 3), only the pallidum demonstrated a statistically significant effect.

We also evaluated the amplitude and statistical significance of CBF variations with ages, shown in Figure 6a Figure 6b, respectively. Interestingly, little spatial overlap is observed between the highest levels of CBF reduction and cortical thinning with age. This is further bolstered by the statistical results (Figure 6c). Controlling for cortical thickness variations on a per-vertex basis did not have a substantial impact on the association between age and CBF, as demonstrated in Figure 6c and 6d.

Reproducibility—The repeated PASL acquisition also facilitated the examination of cross-run CBF measurement repeatability in the same scan session. We found a mean CBF estimation difference of ≅7% (of group-mean) between scans, with no significant variation across cortical and subcortical structures. Furthermore, to determine the reliability of the observed regional CBF decreases, we divided the dataset into two samples, matched for both age and sex, with the first sample used to identify ROIs exhibiting significant age-associated CBF reduction (See Methods). The ROIs were subsequently used to test for similar effects in the second sample, as described in our prior work (Salat et al., 2004; Salat et al., 2009; Dickerson et al., 2008). Significant regional CBF decline with age was robustly observed across these independent samples (see Supplementary Materials), as were the patterns of age-associated cortical thinning.

CBF and Cortical Thickness Interactions—Cortical thinning was found to be largely bilateral, though stronger in the right hemisphere. Qualitative examination of potential mechanisms via various interactions between CBF and cortical thickness is presented in Figure 7, including,

1. The overlap of regions showing age-associated decline in cortical thickness and in CBF (Figure 7a) was used to address whether cortical thinning result from changes in CBF or vice versa), and we found that cortical thinning did not substantially overlap with regions showing the most notable CBF reductions;
2. The overlap between regions showing age-effects in CBF and high regional CBF in the young controls (Figure 7b) was used to assess whether CBF decline later in life are driven by spatial bias early in life, and we found this link to be limited to the temporal, parietal and precuneus regions;
3. The overlap between regions of high CBF in young adults and those showing associations between cortical thickness and age (Figure 7c) was used to assess whether high resting CBF was related to predisposition for cortical thinning, and substantial overlap was observed;
4. The coexistence of age-associations in CBF and high cortical thickness in young adults (Figure 7d) was used to assess if changes in CBF occur selectively in thicker or thinner regions of cortex, and we found regions of reduced CBF not to be directly associated with thickness.

DISCUSSION

This study investigated the relationship between cerebral perfusion and aging. Reproducibility associated with pulsed ASL CBF measurements is in agreement with previous findings (Jiang et al., 2010; Parkes et al., 2004). We demonstrated substantial spatial non-uniformity in CBF cortically and subcortically, independent of age. Significant age-associated regional CBF reduction was widely observed throughout the cortex. Importantly, these reductions were not closely associated with age-related cortical thinning. In contrast, a suggestive relationship was found between CBF in young adults and cortical thinning in aging. This potential link to mechanisms of age-associated atrophy is of interest for future examination. Given previous evidence of an important relationship between pathological perfusion reduction and neuronal degeneration (Fierstra et al., 2010), the current findings may indicate a distinct paradigm characteristic of normal aging. Lastly, the spatial distribution of CBF reductions spans regions reported to be involved in default-mode activity (for review see (Raichle and Snyder, 2007)), warranting further investigation.

CBF Reduction in Aging

Our CBF estimates are consistent with values in the PET and MRI literature (Calamante et al., 1999; Čavuşoğlu et al., 2009; Leenders et al., 1990; Shin et al., 2007), and particularly with prior findings using ASL (Wong et al., 1998 -a, b; Ye et al., 1997; Zou et al., 2009). The loci of low and high perfusion are in agreement with numerous reports using PET (Ishii et al., 1996; Leenders et al., 1990; Raichle et al., 2001) and CASL (Lee et al., 2009; Zou et al., 2009).

The inter-group comparisons of mean CBF in parcellations revealed more regions with age-related CBF decrease than did the per-vertex surface-regression analyses. In fact, the use of the two approaches served as self check for consistency, and we found aging-associated cortical CBF reduction to be greatest later in life (after the transition from middle-aged to older-adults) instead of being a linear process. Nonetheless, our data is under-powered for demonstrating significant nonlinear trends, given the inter-subject variability.

Reproducible cross-sectional age-effects in CBF were demonstrated with negligible cohort differences between, the localization of which corresponding to a superset of regions implicated in aging in previous $H_2{}^{15}O$ PET and CASL studies, including the frontal and insular cortices (Leenders et al., 1990), the frontal-temporal region (Beason-Held et al., 2009; Inoue et al., 2005; Lee et al., 2009; Pagani et al., 2002), the precuneus (Beason-Held et al., 2009; Lee et al., 2009), and the anterior cingulate (Pagani et al., 2002). The left hemisphere was associated with a greater number of regions with reduced CBF than the right hemisphere, specifically the lateral occipital and supramarginal regions, in agreement with PET findings (Pagani et al., 2002), though there was little hemispheric bias in the rates of CBF reduction.

Our measurements of the CBF-age relationship in the frontal and insular regions are in excellent agreement with observations by Leenders *et al.*, while those in the superior frontal region and precuneus are in agreement with longitudinal findings by Beason-Held *et al.* (Beason-Held et al., 2009). The CBF decline in the frontal, temporal, and parietal regions are macroscopically in agreement with CT findings both cross-sectionally and longitudinally (Akiyama et al., 1997), although Akiyama *et al.* noted an absence of longitudinal effects in the occipital lobe, in contrast to their cross-sectional results and to our own results. Also, our finding of reduced CBF in the superior parietal region is in contrast with reports by Beason-Held *et al.* (Beason-Held et al., 2009), potentially as the latter was a longitudinal study focusing on an age-range truncated to involve only older adults (age = 68.4 ± 6.8 years). A

key future goal will be to study the potential disparities between longitudinal and cross-sectional assessments.

In the subcortex, our observation of reduced perfusion in the caudate and thalamus in the OA is consistent with CT findings (Akiyama et al., 1997), although unlike Akiyama *et al.*, we did not observe significant CBF-age relationship in the putamen. Finally, despite prior findings of augmented subcortical perfusion in healthy older adults (Lee et al., 2009; Pagani et al., 2002), such increases with age were not found in the present setting; such effects may be attributed to partial-volume contamination (Barnden et al., 2005). It should be noted, however, that prior SPECT studies examined CBF normalized by global flow, implying that an unchanged subcortical CBF may seem to be an increase, should global CBF be reduced.

In terms of mean cortical CBF, the sex-difference was only significant in the older adults, perhaps owing to the substantial inter-subject variability within groups. CBF disparities between genders spatially selective, with women consistently being associated with higher CBF, also in accordance with prior results (Jones et al., 1998; Li et al., 2004; Parkes et al., 2004; Shin et al., 2007). As to the slope of CBF vs. age, no significant gender bias was found, echoing previously findings in whole-brain analyses (Buijs et al., 1998), but contrary to select PET and MRI experiments (Pagani et al., 2002; Shin et al., 2007).

The currently observed whole-cortex CBF reduction of ~0.38% per year is lower than previously reported whole-brain (~0.52% per year, using 2D phase-contrast cerebral angiography) (Buijs et al., 1998) and whole-cortical measurements (0.76% per year, using contrast-enhanced MRI) (Shin et al., 2007), but more comparable with CASL-based findings (Parkes et al., 2004). Several factors may contribute to the differences, including the inclusion of white matter in the estimation of whole-head perfusion and the subject selection criteria (such as the inclusion of individuals with cognitive deficits and/or macrovascular pathology). In addition, previous studies have been more limited in slope, owing in part to the invasive nature of traditional perfusion imaging techniques -- the non-invasiveness and high accessibility of pulsed ASL imaging was integral to achieving comprehensiveness in our cohort. Moreover, earlier perfusion quantification techniques were sensitive to limitations in temporal (Chen et al., 2005a; Østergaard et al., 1996) and spatial resolution (Chen et al., 2005b; Inoue et al., 2005; Inoue et al., 2003; Law et al., 2000; Meltzer et al., 2000). From the latter perspective, the effect of atrophy is of particular importance to aging studies, and the interpretation of CBF changes is ideally made in conjunction with structural changes.

Knowledge of the patterns of age-associated CBF decline is invaluable for distinguishing normal changes from more detrimental disease-related degeneration. While much of our findings resemble SPECT-based observations in dementia (Matsuda et al., 2002; Matsuda et al., 2003) and more recently using CASL (Dai et al., 2009; Hayasaka et al., 2006; Nagata et al., 2000; Schuff et al., 2009; Shimizu et al., 2010; Yang et al., 2002) and AD (Tosun et al., 2010), some exceptions were found, such as in the amygdala (Dai et al., 2009) and hippocampus (Alsop et al., 2008; Dai et al., 2009; Fleisher et al., 2009; Heo et al., 2010; Ito et al., 2006; Nagata et al., 2000).

Association between CBF Reductions and Tissue Atrophy

The spatial distribution of cortical thinning with age in the current cohort was robustly observed across independent samples, and in agreement with previous reports based on both MRI (Fjell et al., 2009; Raz et al., 1997; Salat et al., 2004) and CT (Akiyama et al., 1997). These results correspond well with those identified by the latter work as exhibiting the most robust cortical thinning. Further agreement was found with other previous MRI-based

findings (Burgmans et al., 2009; Raz et al., 2003; Sullivan et al., 2004; Walhovd et al., 2005), although the shrinkage was less pronounced than previously reported.

Based on prior knowledge linking perfusion deficit and tissue damage (Fierstra et al., 2010; Koehler et al., 2009), we hypothesized that CBF reduction and tissue atrophy would be closely related in aging. However, a key finding of this work is to the contrary. Specifically, although regions which exhibit significant cortical thinning, such as the frontal, temporal and precuneus regions, also exhibit reduced perfusion, in agreement with findings by Tosun *et al.* (Tosun et al., 2010), there were many regions showing reduced cortical thickness without a concomitant reduction in CBF. Furthermore, the association between CBF and age was minimally influenced by neutralizing the effect of cortical thinning. This relative dissociation of CBF reduction and atrophy in aging builds upon potentially related observations in healthy older adults examined with PET by Sojkova *et al.* (Sojkova et al., 2010) but are not consistent with earlier CT results in aging (Akiyama et al., 1997; Obara et al., 1994). The times of occurrence of CBF and tissue volume reductions are likely to differ, the significance thereof remaining to be clarified.

Stemming from neurovascular coupling requirements, the influence of age on CBF is likely to reflect underlying changes in neuronal activity. Age-related and comparable decreases in CBF and $CMRO_2$ have been reported previously (Leenders et al., 1990; Pantano et al., 1984), particularly in the parietal (Burns and Tyrrell, 1992), frontal and temporal lobes (Burns and Tyrrell, 1992; Leenders et al., 1990), coinciding with locations showing CBF reduction in this study. It is unclear whether basal flow and/or metabolism are related to resistance to cerebrovascular degeneration in aging/dementia. Our results qualitatively demonstrate a parallel between reduced CBF and elevated resting oxidative metabolism (Buckner et al., 2005; Gjedde et al., 2005; Raichle et al., 2001), a set of regions widely referred to as part of the default-mode network. The significance of this finding will be further investigated. Finally, the development of hyper- or hypotension, particular in the MA and OA populations, has been suggested as a contributor to CBF changes (Alves and Busatto, 2006; Gruhn et al., 2001).

While the relationship between concurrently observed CBF reduction and cortical atrophy has previously been investigated using a voxel-based morphometric (VBM) approach, existing VBM results have not been consistent (Ito et al., 2006; Van Laere and Dierckx, 2001), perhaps due to such limiting factors as spatial resolution and common uncertainties in the accuracy of volume-based registration for atlas-based analyses (Greve and Fischl, 2009; Zollei et al., 2010), particularly in view of complications introduced by age-related atrophy (Dai et al., 2008a). Our findings build upon prior work by Tosun *et al.*, in which surface mapping was used to demonstrate dissociations between CBF and cortical thickness reductions in individuals with AD (Tosun et al., 2010). We did not compensate the CBF values themselves for intra-voxel tissue heterogeneity (Asllani et al., 2008), but instead regressed out the contribution of grey-matter volume variations from the association between CBF and age. Finally, our results are based on the largest perfusion and structural MRI datasets acquired to-date for such investigations on aging, and the outcome of our surface-based group-analyses was further confirmed by the results of our subject-specific native-space volume-based ROI-analyses.

Limitations and Caveats

Pulsed ASL is known for its sensitivity to arterial-transit delay, which may be lengthened in aging. In addition, in the healthy subjects, the inferior half of the brain is reportedly associated with longer transit delays (Qiu et al., 2010), while relatively long delays have also been associated the frontal and occipital lobes (MacIntosh et al., 2010). As these factors are important determinants of CBF accuracy, our PASL parameters were chosen to minimize

velocity-related bias. Specifically, a relatively short TI_1 of 600 ms facilitated the minimization of bolus-width sensitivity even for rapid flow, common to younger subjects, while a TI_2 of 1600 ms exceeds the longest grey-matter transit delay (cortical and subcortical) expected in healthy adults (Qiu et al., 2010), accommodating the slower flow which may be expected in certain older adults. Furthermore, the cortical and subcortical CBF reduction patterns in aging observed in this study differ spatially from the patterns of transit delay heterogeneity. Thus, it is not likely that the observed changes are driven primarily by the above PASL-related artifacts and biases, although it is possible that arterial transit times may contribute in some way to the reported effects. Additionally, ASL measures of CBF are dependent on tissue and blood T_1 and T_2^*. These parameters have been found to decrease with advancing age in brain tissue (Cho et al., 1997; Mitsumori et al., 2009). Based on these prior findings, we estimated the worst-case errors using numerical simulations (data not shown), and found these figures to translate to a CBF underesmation of up to ~10% (T_2-related) and CBF overestimation of up to ~8% (T_1-related), respectively. Notwithstanding, these opposite and competing effects are exceeded by the CBF reductions currently reported. Nonetheless, prospectively, we hope to study the effect of physiological changes in aging on CBF measurement (Wu et al., 2009), and to enhance the sensitivity of our CBF measures using novel pseudo-continuous ASL techniques (Xu et al., 2010).

Importantly, the current study presents a cross-sectional view on aging. We are aware of the potential confounds of cross-sectional studies, such as cohort effects. To assess the potential influence of cohort effects, we have repeated the analyses on two independent sample populations, and arrive at similar results. Furthermore, our results are compatible with previous longitudinal findings (Sojkova et al., 2008), although we noted slight discrepancies partially due to differences in the subjects' age range. More detailed examinations of the comparability of cross-sectional to longitudinal findings will be one of the key targets for future efforts.

Conclusions

An accurate understanding of cerebral perfusion changes in normal aging is key to deciphering the neurovascular manifestations and pathogenesis of age-related neurological diseases. This work is the first instance in which surface processing procedures are used to map in detail MR measures of perfusion and structural changes associated with normal aging. We have demonstrated regionally specific grey matter perfusion variations across the adult lifespan using pulsed ASL. Our results demonstrate that regions of CBF reduction are largely distinct from those most burdened by grey-matter atrophy, suggesting differential contributions to age-related cognitive decline by hemodynamic and structural changes. Furthermore, the age-associated CBF decreases were most significant in regions commonly associated with higher resting metabolism. This work sets the stage for a larger scale use of pulsed ASL to investigate perfusion alterations in cerebrovascular disease and dementia.

Supplementary Material

Refer to Web version on PubMed Central for supplementary material.

Acknowledgments

This research was supported by NIH grants K01AG024898, R01NR010827, NS042861, and P41RR14075, as well as the Canadian Institutes of Health Research (CIHR) and the Athinoula A. Martinos Center for Biomedical Imaging. We also thank Dr. Doug Greve for his input on multi-modal image registration.

References

Aguero-Torres H, Kivipelto M, von Strauss E. Rethinking the dementia diagnoses in a population-based study: What is Alzheimer's disease and what is vascular dementia? A study from the Kungsholmen project. Dementia and Geriatric Cognitive Disorders. 2006; 22:244–249. [PubMed: 16902279]

Akiyama H, Meyer JS, Mortel KF, Terayama Y, Thornby JI, Shizuko K. Normal human aging: factors contributing to cerebral atrophy. Journal of the Neurological Sciences. 1997; 152:39–49. [PubMed: 9395125]

Alsop DC, Casement M, de Bazelaire C, Fong T, Press DZ. Hippocampal hyperperfusion in Alzheimer's disease. NeuroImage. 2008; 42:1267–1274. [PubMed: 18602481]

Alsop DC, Dai W, Grossman M, Detre JA. Arterial spin labeling blood flow MRI: its role in the early characterization of Alzheimer's disease. J Alzheimers Dis. 2010; 20:871–880. [PubMed: 20413865]

Alves TC, Busatto GF. Regional cerebral blood flow reductions, heart failure and Alzheimer's disease. Neurological Research. 2006; 28:579–587. [PubMed: 16945208]

Asllani I, Borogovac A, Brown TR. Regression algorithm correcting for partial volume effects in arterial spin labeling MRI. Magn Reson Med. 2008; 60:1362–1371. [PubMed: 18828149]

Barnden LR, Behin-Ain S, Kwiatek R, Casse R, Yelland L. Age related preservation and loss in optimized brain SPECT. Nuclear Medicine Communications. 2005; 26:497–503. [PubMed: 15891592]

Beason-Held LL, Kraut MA, Resnick SM. Stability of default-mode network activity in the aging brain. Brain Imaging Behav. 2009; 3:123–131. [PubMed: 19568331]

Bell RD, Zlokovic BV. Neurovascular mechanisms and blood-brain barrier disorder in Alzheimer's disease. Acta Neuropathologica. 2009; 118:103–113. [PubMed: 19319544]

Breteler MM. Vascular risk factors for Alzheimer's disease: An epidemiologic perspective. Neurobiology of Aging. 2000; 21:153–160. [PubMed: 10867200]

Buckner RL, Head D, Parker J, Fotenos AF, Marcus D, Morris JC, Snyder AZ. A unified approach for morphometric and functional data analysis in young, old and demented adults using automated atlas-based head size normalization: reliability and validation against manual measurement of total intracranial volume. NeuroImage. 2004; 23:724–738. [PubMed: 15488422]

Buckner RL, Snyder A, Shannon BJ, LaRossa G, Sachs R, Fotenos AF, Sheline YI, Klunk WE, Mathis CA, Morris JC, Mintun MA. Molecular, structural, and functional characterizatioin of Alzheimer's disease: evidence for a relationship between default activity, amyloid, and memory. Neurobiology of Aging. 2005; 25:7709–7717.

Buijs PC, Krabbe-Hartkamp MJ, Bakker CJ, de Lange EE, Ramos LM, Breteler MM, Mali WP. Effect of age on cerebral blood flow: measurement with ungated two-dimensional phase-contrast MR angiography in 250 adults. Radiology. 1998; 209:667–674. [PubMed: 9844657]

Burgmans S, van Boxtel MP, van den Berg KE, Gronenschild EH, Jacobs HI, Jolles J, Uylings HB. The posterior parahippocampal gyrus is preferentially affected in age-related memory decline. Neurobiology of Aging. 2009 Epub ahead of print.

Burns A, Tyrrell P. Association of age with regional cerebral oxygen utilization: a positron emission tomography study. Brain. 1992; 21:316–320.

Buxton RB, Frank LR, Wong EC, Siewert B, Warach S, Edelman RR. A general kinetic model for quantitative perfusion imaging with arterial spin labeling. Magn Reson Med. 1998; 40:383–396. [PubMed: 9727941]

Calamante F, Thomas DL, Pell GS, Wiersma J, Turner R. Measuring cerebral blood flow using magnetic resonance imaging techniques. J Cereb Blood Flow Metab. 1999; 19:701–735. [PubMed: 10413026]

Caroli A, Testa C, Geroldi C, Nobili F, Barnden LR, Guerra UP, Bonetti M, Frisoni GB. Cerebral perfusion correlates of conversion to Alzheimer's disease in amnestic mild cognitive impairment. Journal of Neurology. 2007; 254:1698–1707. [PubMed: 17990057]

Çavuşoğlu M, Pfeuffer J, Uğurbil K, Uludağ K. Comparison of pulsed arterial spin labeling encoding schemes and absolute perfusion quantification. Magnetic Resonance Imaging. 200910.1016/j.mri.2009.04.002

Chen JJ, Smith MR, Frayne R. The advantages of frequency domain modeling in DSC MR CBF quantification. Magn Reson Med. 2005a; 53:700–707. [PubMed: 15723395]

Chen JJ, Smith MR, Frayne R. Partial-volume effects in DSC MR perfusion quantification. J Magn Reson Imaging. 2005b; 22:390–399. [PubMed: 16104009]

Cho S, Jones DK, Reddick WE, Ogg RJ, Steen RG. Establishing norms for age-related changes in proton T1 of human brain tissue in vivo. Magn Reson Imaging. 1997; 15:1133–1143. [PubMed: 9408134]

Dai W, Carmichael OT, Lopez OL, Becker JT, Kuller LH, Gach HM. Effects of image normalization on the statistical analysis of perfusion MRI in elderly adults. J Magn Reson Imaging. 2008a; 28:1351–1360. [PubMed: 19025942]

Dai W, Garcia D, De Bazelaire C, Alsop DC. Continuous flow-driven inversion for arterial spin labeling using pulsed radio frequency and gradient fields. Magn Reson Med. 2008b; 60:1488–1497. [PubMed: 19025913]

Dai W, Lopez OL, Carmichael OT, Becker JT, Kuller LH, Gach HM. Abnormal regional cerebral blood flow in cognitively normal elderly subjects with hypertension. Stroke. 2008c; 39:349–354. [PubMed: 18174483]

Dai W, Lopez OL, Carmichael OT, Becker JT, Kuller LH, Gach HM. Mild cognitive impairment and alzheimer disease: patterns of altered cerebral blood flow at MR imaging. Radiology. 2009; 250:856–866. [PubMed: 19164119]

de la Torre JC. Is Alzheimer's disease preceded by neurodegeneration or cerebral hypoperfusion? Annals of Neurology. 2005; 57:783–784. [PubMed: 15929049]

Detre, JA.; Alsop, DC.; Samuels, OB.; Gonzalez-Atavales, J.; Raps, EC. Departments of Neurology and Radiology, University of Pennsylvania; Philadeplphia, Pennyslvania., Sydney: 1998. Cerebravascular reserve testing using perfusion MRI with arterial spin labeling in normal subjects and patients with cerebrovascualr disease.

Detre JA, Alsop DC, Vives LR, Maccotta L, Teener JW, Raps EC. Noninvasive MRI evaluation of cerebral blood flow in cerebrovascular disease. Neurology. 1998; 50:633–641. [PubMed: 9521248]

Detre, JA.; Leigh, JS.; Williams, DS.; Koretsky, AP. Perfusion imaging Metabolic Magnetic Resonance Research Center. University of Pennsylvania School of Medicine; Philadelphia: 1992. p. 19104

Detre JA, Zhang W, Roberts DA, Silva AC, Williams DS, Grandis DJ, Koretsky AP, Leigh JS. Tissue specific perfusion imaging using arterial spin labeling NMR in Biomedicine. 1994; 7:75–82.

Dickstein DL, Walsh J, Brautigam H, Stockton SD Jr, Gandy S, Hof PR. Role of vascular risk factors and vascular dysfunction in Alzheimer's disease. Mount Sinai Journal of Medicine. 2010; 77:82–102. [PubMed: 20101718]

Driscoll I, Zhou Y, An Y, Sojkova J, Davatzikos C, Kraut MA, Ferrucci L, Mathis CA, Klunk WE, Wong DF, Resnick SM. Lack of association between ^{11}C-PiB and longitudinal brain atrophy in non-demented older individuals. Neurobiology of Aging. 201010.1016/j.neurobiolaging.2009.12.008

Duron E, Hanon O. Antihypertensive treatments, cognitive decline, and dementia. J Alzheimers Dis. 2010 [Epub ahead of print].

Elias MF, D'Agostino RB, Elias PK, Wolf PA. Neuropsychological test performance, cognitive functioning, blood pressure, and age: the Framingham Heart Study. Experimental Aging Research. 1995; 21:369–391. [PubMed: 8595803]

Farmer ME, Kittner SJ, Abbott RD, Wolz MM, Wolf PA, White LR. Longitudinally measured blood pressure, antihypertensive medication use, and cognitive performance: the Framingham Study. Journal of Clinical Epidemiology. 1990; 43:475–480. [PubMed: 2324788]

Fierstra J, Poublanc J, Han JS, Silver F, Tymianski M, Crawley AP, Fisher JA, Mikulis DJ. Steal physiology is spatially associated with cortical thinning. Journal of Neurology, Neurosurgery and Psychiatry. 2010; 81:290–293.

Fischl B, Dale AM. Measuring the thickness of the human cerebral cortex from magnetic resonance images. Proceedings of the National Academy of Sciences of the United States of America. 2000; 97:11050–11055. [PubMed: 10984517]

Fischl B, Rajendran N, Busa E, Augustinack J, Hinds O, Yeo BT, Mohlberg H, Amunts K, Zilles K. Cortical folding patterns and predicting cytoarchitecture. Cereb Cortex. 2008; 18:1973–1980. [PubMed: 18079129]

Fischl B, Salat DH, van der Kouwe AJW, Makris N, Segonne F, Quinn BT, Dale AM. Sequence-independent segmentation of magnetic resonance images. NeuroImage. 2004a; 23:S69–S84. [PubMed: 15501102]

Fischl B, Sereno MI, Dale AM. Cortical surface-based analysis. II: Inflation, flattening, and a surface-based coordinate system. NeuroImage. 1999a; 9:195–207. [PubMed: 9931269]

Fischl B, Sereno MI, Tootell RB, Dale AM. High-resolution intersubject averaging and a coordinate system for the cortical surface. Hum Brain Mapp. 1999b; 8:272–284. [PubMed: 10619420]

Fischl B, van der Kouwe A, Destrieux C, Halgren E, Segonne F, Salat DH, Busa E, Seidman LJ, Goldstein J, Kennedy D, Carviness V, Makris N, Rosen B, Dale AM. Automatically parcellating the human cerebral cortex. Cereb Cortex. 2004b; 14:11–22. [PubMed: 14654453]

Fjell AM, Westlye LT, Amlien I, Espeseth T, Reinvang I, Raz N, Agartz I, Salat DH, Greve DN, Fischl B, Dale AM, Walhovd KB. High consistency of regional cortical thinning in aging across multiple samples. Cereb Cortex. 2009; 19:2001–2012. [PubMed: 19150922]

Fleisher AS, Sherzai A, Taylor C, Laugbaum JBS, Chen K, Buxton RB. Resting-state BOLD networks versus task-associated functional MRI for distinguishing Alzheimer's disease risk groups. NeuroImage. 2009; 47:1678–1690. [PubMed: 19539034]

Folstein MF, Folstein SE, McHugh PR. "Mini-mental state". A practical method for grading the cognitive state of patients for the clinician. Journal of Psychiatric Research. 1975; 12:189–198. [PubMed: 1202204]

Forette F, Seux ML, Staessen JA, Thijs L, Babarskiene MR, Babeanu S, Bossini A, Fagard R, Gil-Extremera B, Laks T, Kobalava Z, Sarti C, Tuomilehto J, Vanhanen H, Webster J, Yodfat Y, Birkenhager WH. Investigators SHiE. The prevention of dementia with antihypertensive treatment: new evidence from the Systolic Hypertension in Europe (Syst-Eur) study. Archives of Internal Medicine. 2002; 162:2046–2052. [PubMed: 12374512]

Genovese CR, Lazar NA, Nichols T. Thresholding of statistical maps in functional neuroimaging using the false discovery rate. NeuroImage. 2002; 15:870–878. [PubMed: 11906227]

Girouard H, Iadecola C. Neurovascular coupling in the normal brain and in hypertension, stroke, and Alzheimer disease. J Appl Physiol. 2006; 100:328–335. [PubMed: 16357086]

Gjedde A, Johannsen P, Cold GE, Østergaard L. Cerebral metabolic response to low blood flow: possible role of cytochrome oxidase inhibition. J Cereb Blood Flow Metab. 2005; 25:1183–1196. [PubMed: 15815583]

Greve DN, Fischl B. Accurate and robust brain image alignment using boundary-based registration. NeuroImage. 2009; 48:68–72.

Grober E, Silwinski M. Development and validation of a model for estimating premorbid verbal intelligence in the elderly. Journal of Clinical and Experimental Neuropsychology. 1991; 13:933–949. [PubMed: 1779032]

Gruhn N, Larsen FS, Boesgaard S, Knudsen GM, Mortensen SA, Thomsen G, Aldershvile J. Cerebral blood flow in patients with chronic heart failure before and after heart transplantation. Stroke. 2001; 11:2530–2533. [PubMed: 11692012]

Gsell W, De Sadeleer C, Marchalant Y, MacKenzie ET, Schumann P, Dauphin F. The use of cerebral blood flow as an index of neuronal activity in functional neuroimaging: experimental and pathophysiological considerations. Journal of Chemical Neuroanatomy. 2000; 20:215–224. [PubMed: 11207420]

Hayasaka S, Du AT, Duarte A, Kornak J, Jahng GH, Weiner MW, Schuff N. A non-parametric approach for co-analysis of multi-modal brain imaging data: Application to Alzheimer's disease. NeuroImage. 2006; 30:768–779. [PubMed: 16412666]

Helenius J, Perkio J, Soinne L, Østergaard L, Carano RAD, Salonen O, Savolainen S, Kaste M, Aronen HJ, Tatlisumak T. Cerebral hemodynamics in a healthy population measured by dynamic susceptibility contrast MR imaging. Acta Radiol. 2003; 44:538–546. [PubMed: 14510762]

Helzner EP, Luchsinger JA, Scarmeas N, Cosentino S, Brickman AM, Glymour MM, Stern Y. Contribution of vascular risk factors to the progression in Alzheimer disease. Archives of Neurology. 2009; 66:343–348. [PubMed: 19273753]

Heo S, Prakash RS, Vossa M, Erickson KI, Ouyang C, Sutton BP, Kramer AF. Resting hippocampal blood flow, spatial memory and aging. Brain Res. 2010; 1315:119–127. [PubMed: 20026320]

Hoge RD, Atkinson J, Gill B, Crelier GR, Marrett S, Pike GB. Linear coupling between cerebral blood flow and oxygen consumption in activated human cortex. Proc Natl Acad Sci U S A. 1999; 96:9403–9408. [PubMed: 10430955]

Inoue K, Ito H, Goto R, Nakagawa M, Kinomura S, Sato T, Sato K, Fukuda H. Apparent CBF decrease with normal aging due to partial volume effects: MR-based partial volume correction on CBF SPECT. Annals of Nuclear Medicine. 2005; 19:283–290. [PubMed: 16097637]

Inoue K, Nakagawa M, Goto R, Kinomura S, Sato T, Sato K, Fukuda H. Regional differences between 99mTc-ECD and 99mTc-HMPAO SPET in perfusion changes with age and gender in healthy adults. Eur J Nucl Med Mol Imaging. 2003; 30:1489–1497. [PubMed: 14579088]

Ishii K, Sasaki M, Kitagaki H, Sakamoto S, Yamaji S, Maeda K. Regional difference in cerebral blood flow and oxidative metabolism in human cortex. Journal of Nuclear Medicine. 1996; 37:1086–1088. [PubMed: 8965174]

Ito H, Inoue K, Goto R, Kinomura S, Taki Y, Okada K, Sato K, Sato T, Kanno I, Fukuda H. Database of normal human cerebral blood flow measured by SPECT: I. Comparison between I-123-IMP, Tc-99m-HMPAO, and Tc-99m-ECD as referred with O-15 labeled water PET and voxel-based morphometry. Annals of Nuclear Medicine. 2006; 20:131–138. [PubMed: 16615422]

Jiang L, Kim M, Chodkowski B, Donahue MJ, Pekar JJ, Van Zijl PCM, Albert M. Reliability and reproducibility of perfusion MRI in cognitively normal subjects. Magn Reson Imaging. 2010; 28:1283–1289. [PubMed: 20573464]

Jones K, Johnson KA, Becker JA, Spiers PA, Albert MS, Holman BL. Use of singular value decomposition to characterize age and gender differences in SPECT cerebral perfusion. Journal of Nuclear Medicine. 1998; 39:965–973. [PubMed: 9627327]

Koehler RC, Roman RJ, Harder DR. Astrocytes and the regulation of cerebral blood flow. Trends in Neurosciences. 2009; 32:160–169. [PubMed: 19162338]

Law I, Iida H, Holm S, Nour S, Rostrup E, Svarer C, Paulson OB. Quantitation of regional cerebral blood flow corrected for partial volume effect using O-15 water and PET: II. Normal values and gray matter blood flow response to visual activation. J Cereb Blood Flow Metab. 2000; 20:1252–1263. [PubMed: 10950384]

Lee C, Lopez OL, Becker JT, Raji C, Dai W, Kuller LH, Gach HM. Imaging cerebral blood flow in the cognitively normal aging brain with arterial spin labeling: implications for imaging of neurodegenerative disease. Journal of Neuroimaging. 2009; 19:344–352. [PubMed: 19292827]

Leenders KL, Perani D, Lammertsma AA, Heather JD, Buckingham P, Healy MJR, Gibbs JM, Wise RJS, Hatazawa J, Herold S, Beaney RP, Brooks DJ, Spinks T, Rhodes C, Frackowiak RS, Jones T. Cerebral blood flow, blood volume and oxygen utilization. Brain. 1990; 113:24–47.

Li ZJ, Matsuda H, Asada T, Ohnishi T, Kanetaka H, Imabayashi E, Tanaka F. Gender difference in brain perfusion 99mTc-ECD SPECT in aged healthy volunteers after correction for partial volume effects. Nuclear Medicine Communications. 2004; 25:999–1005. [PubMed: 15381867]

Lu H, Donahue MJ, van Zijl PCM. Detrimental effects of BOLD signal in arterial spin labeling fMRI at high field strength. Magn Reson Med. 2006; 56:546–552. [PubMed: 16894581]

MacIntosh BJ, Filippini N, Chappell MA, Woolrich MW, Mackay CE, Jezzard P. Assessment of arterial arrival times derived from multiple inversion time pulsed arterial spin labeling MRI. Magn Reson Med. 2010; 63:641–647. [PubMed: 20146233]

Matsuda H, Kanetaka H, Ohnishi T, Asada T, Imabayashi E, Nakano S, Katoh A, Tanaka F. Brain SPET abnormalities in Alzheimer's disease before and after atrophy correction. Eur J Nucl Med Mol Imaging. 2002; 29:1502. [PubMed: 12397471]

Matsuda H, Ohnishi T, Asada T, Li ZJ, Kanetaka H, Imabayashi E, Tanaka F, Nakano S. Correction for partial-volume effects on brain perfusion SPECT in healthy men. Journal of Nuclear Medicine. 2003; 44:1243–1252. [PubMed: 12902414]

Meltzer CC, Cantwell MN, Greer PJ, Ben-Eliezer D, Smith G, Frank G, Kaye WH, Houck PR, Price JC. Does cerebral blood flow decline in healthy aging? A PET study with partial-volume correction. Journal of Nuclear Medicine. 2000; 41:1842–1848. [PubMed: 11079492]

Meyer JS, Takashima S, Terayama Y, Obara K, Muramatsu K, Weathers S. CT changes associated with normal aging of the human brain. Journal of the Neurological Sciences. 1994; 123:200–208. [PubMed: 8064316]

Mitsumori F, Watanabe H, Takaya N. Estimation of brain iron concentration in vivo using a linear relationship between regional iron and apparent transverse relaxation rate of tissue water at 4.7 T. Magn Reson Med. 2009; 62:1326–1330. [PubMed: 19780172]

Morrison JH, Hof PR. Life and death of neurons in the aging brain. Science. 1997; 278:412–419. [PubMed: 9334292]

Nagata K, Maruya H, Yuya H, Terashi H, Mito Y, Kato H, Sato M, Satoh Y, Watahiki Y, Hirata Y, Yokoyama E, Hatazawa J. Can PET data differentiate Alzheimer's disease from vascular dementia? Annals of the New York Academy of Sciences. 2000; 903:252–261. [PubMed: 10818514]

Obara K, Meyer JS, Motel KF, Muramatsu K. Cognitive declines correlate with decreased cortical volume and perfusion in dementia of Alzheimer type. Journal of the Neurological Sciences. 1994; 127:96–102. [PubMed: 7699398]

Oguz KK, Golay X, Pizzini FB, Freer CA, Winrow N, Ichord R, Casella JF, Zijl PCMv, Melhem ER. Sickle cell disease: continuous arterial spin-labeling perfusion MR imaging in children. Radiology. 2003; 227:567–574. [PubMed: 12663827]

Østergaard L, Weisskoff RM, Chesler DA, Gyldensted C, Rosen BR. High resolution measurement of cerebral blood flow using intravascular tracer bolus passages. Part I: Mathematical approach and statistical analysis. 1996; 36:715–725.

Pagani M, Salmaso D, Jonsson C, Hatherly R, Jacobsson H, Larsson SA, Wägner A. Regional cerebral blood flow as assessed by principal component analysis and (99m)Tc-HMPAO SPET in healthy subjects at rest: normal distribution and effect of age and gender. Eur J Nucl Med Mol Imaging. 2002; 29:67–75. [PubMed: 11807609]

Pantano P, Baron JC, Lebrun-Grandié P, Duquesnoy N, Bousser MG, Comar D. Regional cerebral blood flow and oxygen consumption in human aging. Stroke. 1984; 15:635–641. [PubMed: 6611613]

Parkes LM, Rashid W, Chard DT, Tofts PS. Normal cerebral perfusion measurements using arterial spin labelign: reproducibility, stability, and age and gender effects. Magn Reson Med. 2004; 51:736–743. [PubMed: 15065246]

Qiu M, Maguire RP, Arora J, Planeta-Wilson B, Weinsimmer D, Wang J, Wang Y, Kim H, Rajeevan N, Huang Y, Carson RE, Constable RT. Arterial transit time effects in pulsed arterial spin labeling CBF mapping: insight from a PET and MR study in normal human subjects. Magn Reson Med. 2010; 63:374–384. [PubMed: 19953506]

Raichle ME, MacLeod AM, Snyder AZ, Powers WJ, Gusnard DA, Shulman GL. A default mode of brain function. Proc Natl Acad Sci U S A. 2001; 98:676–682. [PubMed: 11209064]

Raichle ME, Snyder AZ. A default mode of brain function: a brief history of an evolving idea. NeuroImage. 2007; 37:1083–1090. [PubMed: 17719799]

Raz N, Gunning FM, Head D, Dupuis JH, McQuain J, Briggs SD, Loken WJ, Thornton AE, Acker JD. Selective aging of the human cerebral cortex observed in vivo: differential vulnerability of the prefrontal gray matter. Cereb Cortex. 1997; 7:268–282. [PubMed: 9143446]

Raz N, Rodrigue KM, Kennedy KM, Head D, Gunning-Dixon F, Acker JD. Differential aging of the human striatum: longitudinal evidence. AJNR American Journal of Neuroradiology. 2003; 24:1849–1856. [PubMed: 14561615]

Rosas HD, Liu AK, Hersch S, Glessner M, Ferrante RJ, Salat DH, van der Kouwe A, Jenkins BG, Dale AM, Fischl B. Regional and progressive thinning of the cortical ribbon in Huntington's disease. Neurology. 2002; 58:695–701. [PubMed: 11889230]

Ruitenberg A, den Heijer T, Bakker SL. Cerebral hypoperfusion and clinical onset of dementia: the Rotterdam Study. Annals of Neurology. 2005; 57:789–794. [PubMed: 15929050]

Sachdev PS, Brodaty H, Looi JC. Vascular dementia: diagnosis, management and possible prevention. Medical Journal of Australia. 1999; 170:81–85. [PubMed: 10026690]

Salat DH, Buckner RL, Snyder AZ, Greve DN, Desikan RS, Busa E, Morris JC, Dale AM, Fischl B. Thinning of the cerebral cortex in aging. Cerebral Cortex. 2004; 14:721–730. [PubMed: 15054051]

Schuff N, Matsumoto S, Kmiecik J, Studholme C, Du A, Ezekiel F, Miller BL, Kramer JH, Jagust WJ, Chui HC, Weiner MW. Cerebral blood flow in ischemic vascular dementia and Alzheimer's disease, measured by arterial spin-labeling magnetic resonance imaging. Alzheimers Dement. 2009; 5:454–462. [PubMed: 19896584]

Segonne F, Dale AM, Busa E, Glessner M, Salat D, Hahn HK, Fischl B. A hybrid approach to the skull stripping problem in MRI. NeuroImage. 2004; 22:1060–1075. [PubMed: 15219578]

Segonne F, Pacheco J, Fischl B. Geometrically accurate topology-correction of cortical surfaces using nonseparating loops. IEEE Trans Med Imag. 2007; 26:518–529.

Shimizu S, Zhang Y, Laxamana J, Miller BL, Kramer JH, Weiner MW, Schuff N. Confordance and discordance between brain perfusion and atrophy in Frontotemporal dementia. Brain Imaging Behav. 2010; 4:46–54. [PubMed: 20503113]

Shin W, Horowitz S, Ragin A, Chen Y, Walker M, Caroll TJ. Quantitative cerebral perfusion using dynamic susceptibility contrast MRI: evaluation of reproducibility and age- and gender-dependence with fully automated image postprocessing algorithm. Magn Reson Med. 2007; 58:1232–1241. [PubMed: 17969025]

Silva AC, Kim SG. Pseudo-continuous arterial spin labeling technique for measuring CBF dynamics with high temporal resolution. Magn Reson Med. 1999; 42:425–429. [PubMed: 10467285]

Skoog I, Lernfelt B, Landahl S, Palmertz B, Andreasson LA, Nilsson L, Persson G, Odén A, Svanborg A. 15-year longitudinal study of blood pressure and dementia. Lancet. 1996; 347:1141–1145. [PubMed: 8609748]

Sled JG, Zijdenbos AP, Evans AC. A nonparametric method for automatic correction of intensity nonuniformity in MRI data. 1998; 17:87–97.

Sojkova J, Beason-Held L, Zhou Y, An Y, Kraut MA, Ye W, Ferrucci L, Mathis CA, Klunk WE, Wong DF, Resnick SM. Longitudinal cerebral blood flow and amyloid deposition: an emerging pattern? Journal of Nuclear Medicine. 2008; 49:1465–1471. [PubMed: 18703614]

Sojkova J, Najjar SS, Beason-Held L, Metter EJ, Davatzikos C, Kraut MA, Zonderman AB, Resnick SM. Intima-media thickness and regional cerebral blood flow in older adults. Stroke. 2010; 41:273–279. [PubMed: 20044526]

Sokoloff L, Reivich M, Kennedy C, des Rosiers MH, Patlak CS, Pettigrew KD, Sakurada O, Shinohara M. The [l4C]deoxyglucose method for the measurement of local cerebral glucose utilization: theory, procedure, and normal values in the conscious and anesthetized albino rat. Journal of Neurochemistry. 1977; 28:897–916. [PubMed: 864466]

Sullivan EV, Rosenbloom M, Serventi KL, AP. Effects of age and sex on volumes of the thalamus, pons, and cortex. Neurobiology of Aging. 2004; 25:185–192. [PubMed: 14749136]

Tohgi H, Yonezawa H, Takahashi S, Sato N, Kato E, Kudo M, Hatano K, Sasaki T. Cerebral blood flow and oxygen metabolism in senile dementia of Alzheimer's type and vascular dementia with deep white matter changes. Neuroradiol. 1998; 40:131–137.

Tosun D, Mojabi P, Weiner MW, Schuff N. Joint analysis of structural and perfusion MRI for cognitive assessment and classification of Alzheimer's disease and normal aging. NeuroImage. 201010.1016/j.neuroimage.2010.04.033

Tzourio C, Anderson C, Chapman N, Woodward M, Neal B, MacMahon S, Chalmers J, Group PC. Effects of blood pressure lowering with perindopril and indapamide therapy on dementia and cognitive decline in patients with cerebrovascular disease. Archives of Internal Medicine. 2003; 163:1069–1075. [PubMed: 12742805]

Uh J, Lewis-Amezcua K, Martin-Cook K, Cheng Y, Weiner M, Diaz-Arrastia R, Devous M Sr, Shen D, Lu H. Cerebral blood volume in Alzheimer's disease and correlation with tissue structural integrity. Neurobiology of Aging. 200910.1016/j.neurobiolaging.2008.12.010

van der Kouwe AJW, Benner T, Salat DH, Fischl B. Brain morphometry with multiecho MPRAGE. NeuroImage. 2008; 40:559–569. [PubMed: 18242102]

Van Laere KJ, Dierckx RA. Brain perfusion SPECT: age- and sex-related effects correlated with voxel-based morphometric findings in healthy adults. Radiol. 2001; 221:810–817.

Vanderploeg RD, Schinka JA, Jones T, Small BJ, Graves AB, Mortimer JA. Elderly norms for the Hopkins Verbal Learning Test-Revised. Clin Neuropsychol. 2000; 14:318–324. [PubMed: 11262707]

Walhovd KB, Fjell AM, Reinvang I, Lundervold A, Dale AM, Eilertsen DE, Quinn BT, Salat DH, Makris N, Fischl B. Effects of age on volumes of cortex, white matter and subcortical strucutures. Neurobiology of Aging. 2005; 26:1261–1270. [PubMed: 16005549]

Wang J, Alsop DC, Li L, Listerud J, Gonzalez-At JB, Schnall MD, Detre JA. Comparison of quantitative perfusion imaging using arterial spin labeling at 1.5 and 4.0 Tesla. Magn Reson Med. 2002; 48:242–254. [PubMed: 12210932]

Williams DS, Detre JA, Leigh JS, Koretsky AP. Magnetic resonance imaging of perfusion using spin inversion of arterial water. Proceedings of the National Academy of Sciences of the United States of America. 1992; 89:212–216. [PubMed: 1729691]

Wong EC, Buxton RB, Frank LR. Implementation of quantitative perfusion imaging techniques for functional brain mapping using pulsed arterial spin labeling. NMR Biomed. 1997; 10:237–249. [PubMed: 9430354]

Wong EC, Buxton RB, Frank LR. A theoretical and experimental comparison of continuous and pulsed arterial spin labeling techniques for quantitative perfusion imaging. 1998; 40:348–355.

Wong EC, Buxton RB, Frank LR. Quantitative imaging of perfusion using a single subtraction (QUIPSS and QUIPSS II). Magn Reson Med. 1998-a; 39:702–708. [PubMed: 9581600]

Wong EC, Buxton RB, Frank LR. A theoretical and experimental comparison of continuous and pulsed arterial spin labeling techniques for quantitative perfusion imaging. 1998-b; 40:348–355.

Wu WC, Edlow BL, Elliot MA, Wang J, Detre JA. Physiological modulations in arterial spin labeling perfusion magnetic resonance imaging. IEEE Trans Med Imag. 2009; 28:703–709.

Xu G, Rowley HA, Wu G, Alsop DC, Shankaranarayanan A, Dowling M, Christian BT, Oakes TR, Johnson SC. Reliability and precision of pseudo-continuous arterial-spin labeling perfusion MRI on 3.0 T and comparison with 15O-water PET in elderly subjects at risk for Alzheimer's disease. NMR Biomed. 2010; 23:286–293. [PubMed: 19953503]

Yang DW, Kim BS, Park JK, Kim SY, Kim EN, Sohn HS. Analysis of cerebral blood flow of subcortical vascular dementia with single photon emission computed tomography: adaptation of statistical parametric mapping. Journal of the Neurological Sciences. 2002; 203–204:199–205.

Ye FQ, Mattay VS, Jezzard P, Frank JA, Weinberger DR, McLaughlin AC. Correction for vascular artifacts in cerebral blood flow values measured by using arterial spin tagging techniques. Magnetic Resonance in Medicine. 1997; 37:226–235. [PubMed: 9001147]

Yesavage JA, Brink TL, Rose TL, Lum O, Huang V, Adey M, Leirer VO. Development and validation of a geriatric depression screening scale: a preliminary report. Psychiatr Res. 1982; 17:37–49.

Zlokovic BV. Neurovascular mechanisms of Alzheimer's neurodegeneration. Trends in Neurosciences. 2005; 28:202–208. [PubMed: 15808355]

Zollei L, Stevens A, Huber K, Kakunoori S, Fischl B. Improved tractography alignment using combined volumetric and surface registration. NeuroImage. 2010; 51:206–213. [PubMed: 20153833]

Zou Q, Wu CW, Stein EA, Zang Y, Yang Y. Static and dynamic characteristics of cerebral blood flow during the resting state. NeuroImage. 2009; 48:515–524. [PubMed: 19607928]

Research Highlights

- First study to map quantitative CBF in normal aging using pulsed arterial-spin labelling
- First study to examine spatial relationship between CBF and cortical thickness changes due specifically to normal aging using surface-based analysis methods
- Grey matter CBF was regional reduced in aging primarily in the cortex
- CBF reductions were not strongly associated with grey-matter atrophy
- Perfusion and structural imaging provide distinct pictures of neuronal health

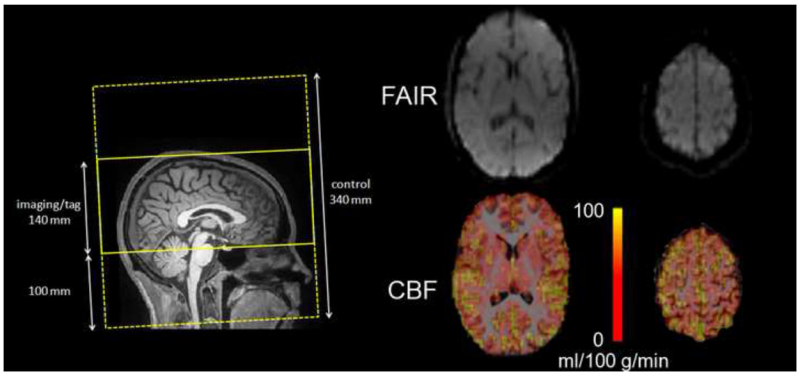

Figure 1.

The tagging and acquisition regions for the PASL scan are illustrated on the left. The PASL raw image and CBF maps (registered to the T1-weighted anatomical images) are shown for an inferior (acquired earlier) and superior (acquire later) slice. The CBF maps demonstrate the expected PASL signal in cortical regions and subcortical grey matter, and low signal in white matter.

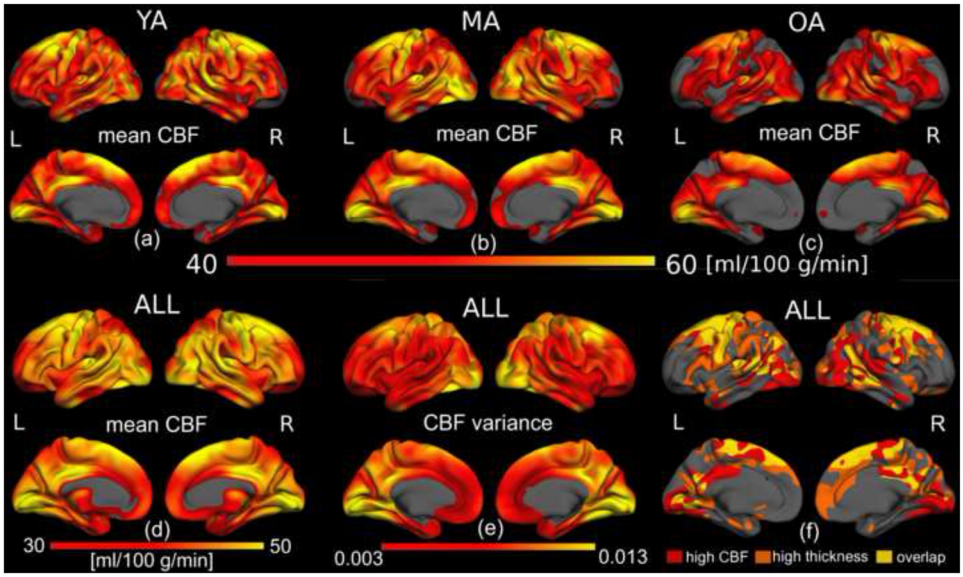

Figure 2.

Quantitative CBF values across the cortex. Average cortical quantitative CBF for the YA (a), MA (b) and OA (c) groups were mapped onto semi-inflated lateral (top) and medial (bottom) surface models. Across all groups, the highest resting CBF was found to be associated mainly with visual and motor areas, in addition to the superior frontal region and the posterior cingulate, confirmed in the average over all subjects (d). The variance in CBF across cortical regions is demonstrated in (e), and may affect the statistical power of age effects. Lastly, the spatial variation in CBF is similar across age-groups, with the older-adults showing visibly reduced CBF. Regions of high mean basal CBF did not directly translate to high cortical thickness (f).

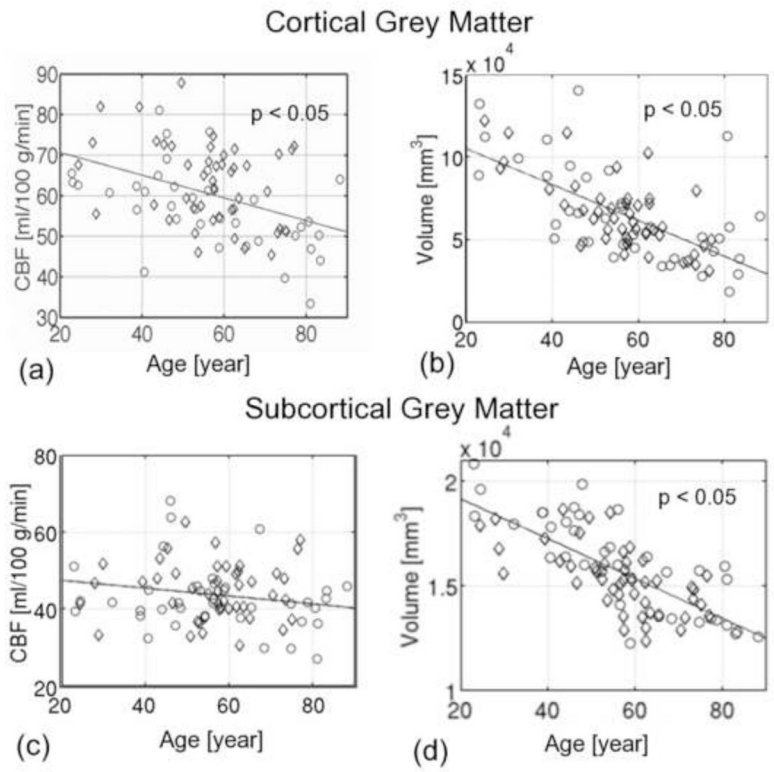

Figure 3.

Association between global cortical CBF, tissue volume and age. Men are indicated by circles and women by diamonds, and regression models are shown as solid lines. The mean CBF across the entire cortex was negatively correlated with age (a), with a slope of −0.38% per year ($p < 0.05$). Cortical grey matter volume, normalized by total intracranial volume, also shows a negative association with age, with a slope of 0.85% per year ($p < 0.05$), exceeding concurrent reductions in CBF. On the other hand, the CBF averaged across all subcortical structures did not significantly vary with age (c), while subcortical grey-matter volume variations were associated with a slope of −0.44% per year ($p < 0.05$). All volume measures were corrected for intracranial volume (eTIV).

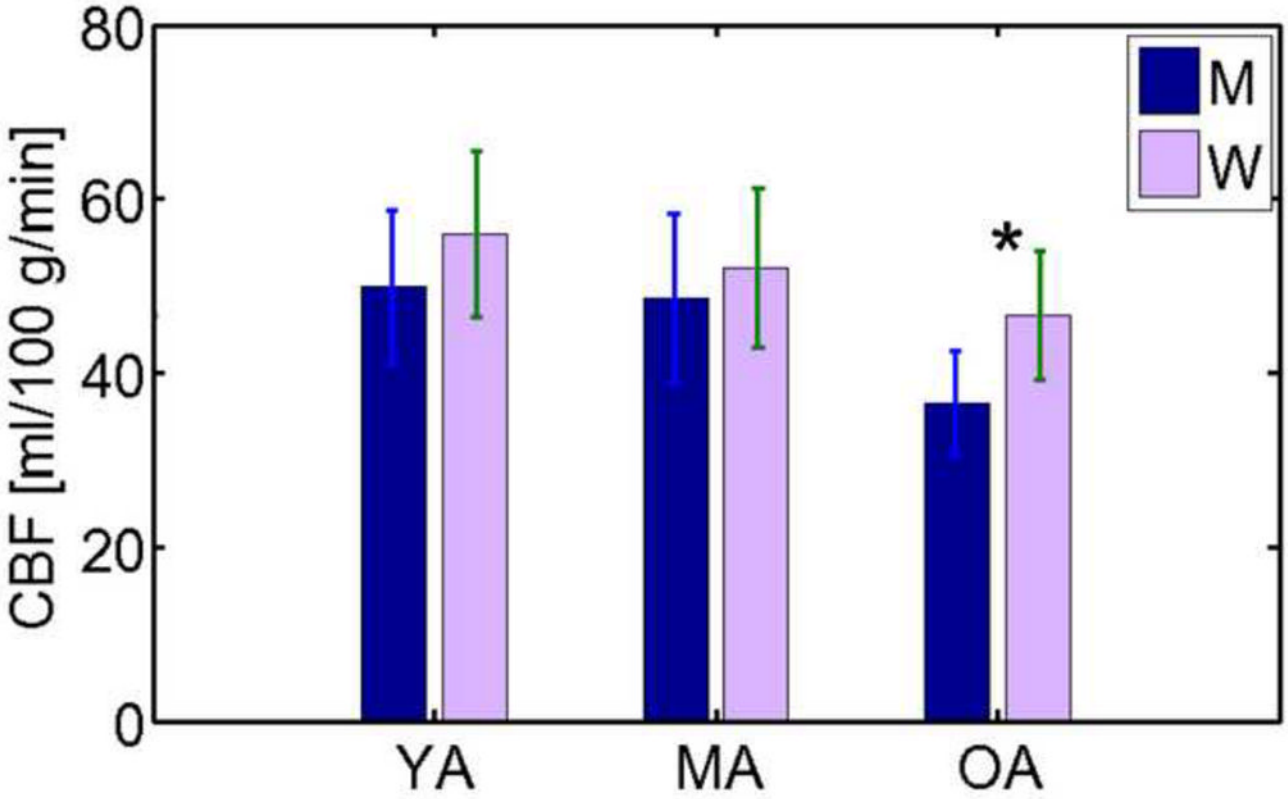

Figure 4.
Global average CBF values in the cortex. Cortical CBF in young (YA), middle aged (MA), and older adults (OA) differentiated by sex (men, M, and women, F). The average CBF across the entire cortex was higher in women in the OA group (denoted by asterisk), but there was no gender-dependence globally in the YA or MA groups. Also evident from this group comparison is a trend for OA to have reduced CBF compared to YA and MA, although the difference eluded statistical significant for either the men or the women.

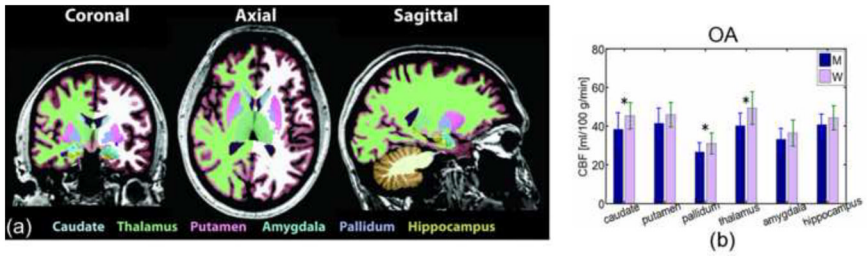

Figure 5.
Mean CBF values in subcortical grey-matter volumes and in the hippocampus, as labelled in (a), demonstrate a difference between men (M) and women (W) for the OA age-group only (b).

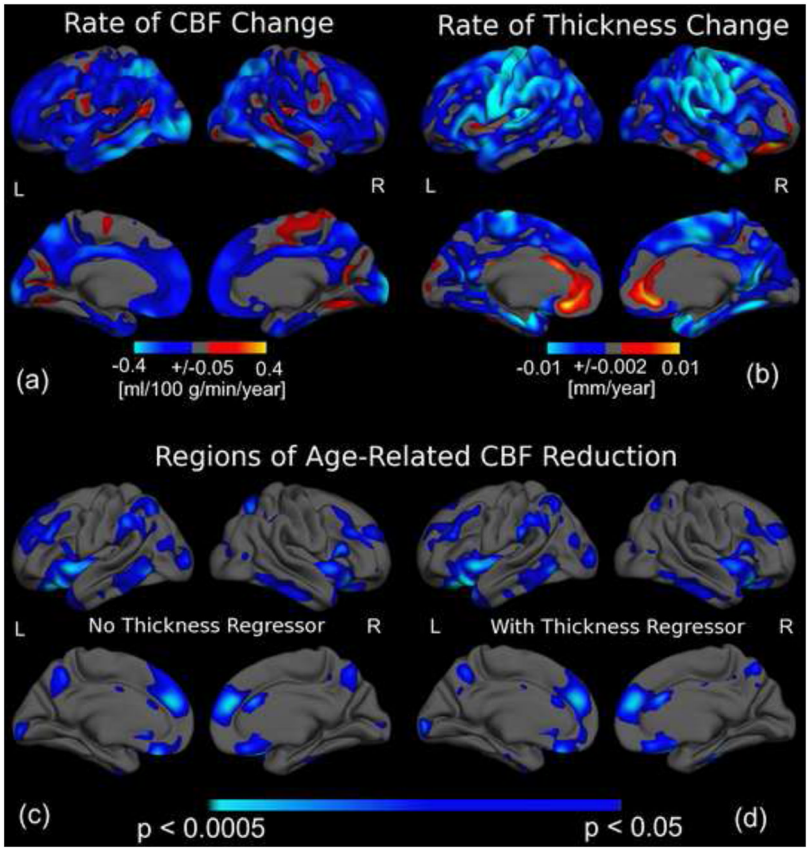

Figure 6.

The association between age and regional CBF as well as cortical thickness. The colour scale in (a) indicates the amplitude of age-associations in CBF, while those in (b) and (c) indicate statistical significance, with light blue and yellow denoting the strongest negative and positive associations, respectively. Regions exhibiting the largest magnitude of CBF reduction (a) and cortical thinning with age (b) did not spatially coincide. The significance map of CBF reductions before (c) and after vertex-wise covariation for age-associations in cortical-thickness (d) only subtly differed. Greatest statistical effects were found in the left supramarginal and occipital gyri, and the right anterior cingulate, as well as bilaterally in the right rostral middle-frontal, superior parietal, middle-inferior temporal and insular regions, medial superior frontal, orbito-frontal and precuneus regions. Furthermore, the localization of regions exhibiting the most rapid age-related CBF decline appeared to coincide with regions showing the highest statistical effects of age on CBF.

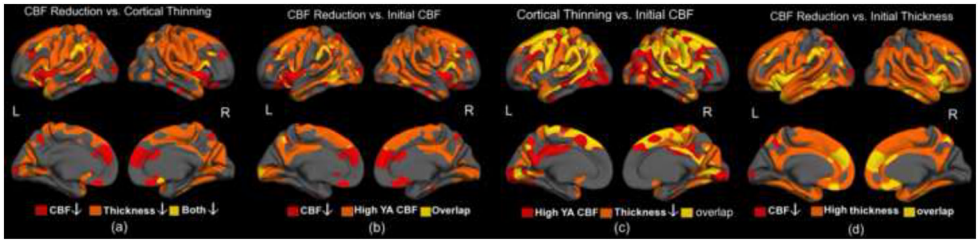

Figure 7.

Associations between resting CBF, cortical thickness and their respective magnitudes of age-association. Regions of high thickness and CBF were defined as those with values exceeding the cortical mean. There was minimal overlap between regions showing age-associated cortical thinning and regions showing age-related decrease in CBF (a). Regions showing the highest CBF in youth (represented by mean CBF in YA group) were not necessarily those showing the greatest cross-sectional age-associated CBF reductions (b). Interestingly, there was substantially more overlap between regions of largest CBF and thickness reductions, although the overlap did not encompass all regions manifesting cortical thinning (c). Finally, almost all regions of high cortical thickness are associated with significant CBF reduction, the latter having been controlled for concurrent thickness decrease (d).

Neuroimage. Author manuscript; available in PMC 2012 September 07.

Table 1

Demographics for young (YA), middle-aged (MA) and older (OA) participants (*MMSE*: Mini-mental Mental Status Exam; *ANART*: National Adult Reading Test; *HVLT*: Hopkins Verbal Learning Test (HVLT); *GDS*: Geriatric Depression Scale; *TRAILS-A&B*: Trail-making Tests A and B).

Group	N	Age [years]			ANART	Education [Years]
		All	Men	Women		
YA	11 (5M/6F)	30.1 ± 6.4	29.3 ± 5.3	30.8 ± 5.6	12.5 ± 8.2	16.1 ± 1.1
MA	38 (16M/22F)	52.0 ± 5.9	51.1 ± 6.3	52.9 ± 5.3	11.8 ± 7.6	16.5 ± 2.8
OA	37 (15M/22F)	70.5 ± 10.4	72.1 ± 8.7	68.3 ± 8.7	12.9 ± 9.0	16.9 ± 2.8

(a)

Metric	Mean for Older Adults (OC)
MMSE	28.1 ± 1.7
ANART	12.9 ± 9.0
HVLT (immediate)	26.0 ± 6.8
TRAILS-A [seconds]	45.5 ± 19.9
TRAILS-B [seconds]	71.7 ± 24.1
GDS	4.0 ± 3.9
Systolic Pressure	122.8 ± 16.1
Diastolic Pressure	76.8 ± 10.1

(b)

Table 2

Group-mean resting CBF values in all cortical parcellations and subcortical structures by cortical hemisphere, cortical hemisphere, and by age-group.

Strucuture		Mean CBF [ml/100 g/min]			Differences				
		YA	MA	OA	Left vs. Right	Men vs. Women	MA vs. YA	OA vs. YA	OA vs. MA
Cortical	Caudal Anterior-Cingulate	45.9 ± 8.8	43.3 ± 10.8	37.0 ± 7.9	L<R*	M<W*			
	Caudal Middle-Frontal	62.8 ± 12.4	56.1 ± 15.7	49.8 ± 15.7	L<R*	M<W*		OA<YA*	OA<MA*
	Cuneus	53.2 ± 6.7	52.2 ± 20.5	39.4 ± 16.5					
	Entorhinal	40.4 ± 17.9	41.9 ± 18.3	33.3 ± 7.9	L<R*	M>W*			
	Fusiform	46.1 ± 9.3	46.6 ± 13.0	39.5 ± 8.4	L>R*				
	Hippocampus	45.7 ± 8.0	48.7 ± 10.0	43.7 ± 8.6	L<R*				
	Inferior Parietal	56.7 ± 9.8	55.2 ± 11.9	44.6 ± 11.9	L>R**	M<W**	MA<YA*	OA<YA*	OA<MA**
	Inferior Temporal	47.1 ± 8.8	43.8 ± 23.2	36.0 ± 14.9					
	Insula	47.7 ± 8.2	47.3 ± 9.4	37.3 ± 8.1	L<R**	M<W*			OA<MA*
	Isthmus Cingulate	58.8 ± 12.4	57.7 ± 16.1	45.4 ± 9.3	L<R**				
	Lateral Occipital	55.2 ± 12.6	57.7 ± 19.9	46.0 ± 13.6	L>R**				
	Lateral Orbitofrontal	46.1 ± 8.5	47.0 ± 10.3	39.8 ± 8.6	L>R**				
	Lingual	53.2 ± 11.4	56.1 ± 12.5	52.2 ± 10.5					
	Medial Orbitofrontal	42.5 ± 7.9	41.6 ± 9.1	34.6 ± 8.4	L>R**				
	Middle Temporal	53.6 ± 9.6	53.0 ± 11.2	44.6 ± 11.0	L<R**				
	Parahippocampal	42.5 ± 12.1	42.4 ± 12.2	36.2 ± 7.6	L<R*				
	Paracentral	52.1 ± 11.7	53.5 ± 10.2	49.5 ± 9.3		M<W*		OA<YA*	OA<MA*
	Parsopercularis	52.2 ± 9.2	49.5 ± 10.4	42.5 ± 9.4	L<R**	M<W*		OA<YA*	OA<MA*
	Parsorbitalis	47.8 ± 8.5	53.7 ± 34.5	40.9 ± 10.5	L>R*			OA<YA*	
	Parstriangularis	53.4 ± 9.7	50.8 ± 11.2	44.2 ± 9.3	L>R**	M<W*			OA<MA*
	Pericalcarine	58.4 ± 7.6	59.8 ± 12.1	52.7 ± 12.3	L>R*	M<W*			OA<MA*
	Postcentral	50.2 ± 10.4	48.9 ± 10.6	42.6 ± 9.2	L<R**	M<W*		OA<YA*	OA<MA*
	Posterior Cingulate	59.9 ± 10.5	55.0 ± 12.0	45.1 ± 11.0	L<R**	M<W**		OA<YA*	OA<MA*

Strucuture		Mean CBF [ml/100 g/min]			Differences				
		YA	MA	OA	Left vs. Right	Men vs. Women	MA vs. YA	OA vs. YA	OA vs. MA
	Precentral	55.2 ± 10.4	54.5 ± 11.7	48.8 ± 9.6	L>R *	M<W *		OA<YA *	OA<MA *
	Precuneus	51.4 ± 8.7	50.0 ± 10.6	43.3 ± 11.5	L<R **	M<W *		OA<YA *	OA<MA *
	Rostral Anterior Cingulate	36.5 ± 5.4	35.4 ± 7.8	31.9 ± 6.7	L>R *				
	Rostral Middle-Frontal	49.3 ± 9.9	45.2 ± 11.3	38.1 ± 11.2	L>R **	M<W **	MA<YA *	OA<YA *	OA<MA *
	Superior Frontal	57.1 ± 8.4	52.9 ± 11.0	46.5 ± 9.4	L>R **	M<W *		OA<YA *	OA<MA *
	Superior Parietal	51.4 ± 12.1	46.3 ± 15.4	35.9 ± 12.4	L<R **	M<W *		OA<YA *	
	Superior Temporal	47.1 ± 9.3	47.4 ± 9.0	42.5 ± 9.3	L<R *	M<W *		OA<YA *	
	Supramarginal	52.7 ± 11.2	49.3 ± 10.0	43.7 ± 7.7	L>R **	M<W **	MA<YA *	OA<YA *	OA<MA *
	Frontal Pole	42.9 ± 9.7	41.0 ± 15.8	33.2 ± 14.2	L>R *	M<W *		OA<YA *	OA<MA *
	Temporal Pole	40.8 ± 9.1	37.4 ± 13.3	35.3 ± 9.6					
	Transverse Temporal	60.7 ± 12.5	64.3 ± 14.1	55.7 ± 15.1					
Mean		**52.6 ± 9.3**	**52.0 ± 10.7**	**42.7 ± 8.8**					
Subcortical	Accumbens	37.1 ± 8.4	37.7 ± 7.4	37.1 ± 9.1					
	Amygdala	36.9 ± 10.6	39.5 ± 9.5	36.1 ± 8.9					
	Caudate	46.1 ± 7.7	44.9 ± 7.1	42.1 ± 8.4	L<R *	M<W **		OA<YA *	OA<MA *
	Pallidum	26.3 ± 6.1	28.4 ± 5.1	28.0 ± 6.7		M<W *		OA<YA *	OA<MA *
	Putamen	46.8 ± 8.2	45.7 ± 7.7	44.7 ± 8.4		M<W *			
	Thalamus	44.8 ± 5.2	47.0 ± 10.4	45.1 ± 9.4				OA<YA *	
Mean		**40.5 ± 7.6**	**41.7 ± 7.1**	**39.5 ± 6.2**					

Note:

* $p < 0.05$,

** $p < 0.00$)

Table 3

Rates of change in CBF (controlling for grey-matter volume as covariate) and cortical thickness in key grey-matter volumes. BOLD figures indicate statistically significant changes.

Structure	Slope of CBF vs. Age [%/year]	*P*	Slope Volume vs. Age [%/year]	*p*
Accumbens	0.23	0.54	**−0.75**	1.4×10^{-6}
Amygdala	−0.10	0.85	**−0.44**	9.2×10^{-8}
Caudate	−0.18	0.13	**−0.35**	0.0041
Pallidum	**−0.05**	0.02	**−0.53**	4.4×10^{-5}
Putamen	−0.06	0.86	**−0.54**	4.4×10^{-10}
Thalamus	−0.11	0.78	**−0.43**	1.0×10^{-11}
Subcortex	−0.09	0.76	**−0.44**	2.7×10^{-14}
Hippocampus	0.04	0.05	**−0.50**	3.1×10^{-10}
Cortex	**−0.38**	0.001	**−0.83**	8.2×10^{-10}